21st Annual Conference of the Canadian Nuclear Society
Toronto, Ontario, Canada / June 11-14, 2000

A MULTIPLE-NODE REAL-TIME PRESSURIZER MODEL

H. Tang
Nuclear Safety Unit
Point Lepreau Generating Station
New Brunswick Power
Canada, E5J 2S6

ABSTRACT

The pressurizer module of the Point Lepreau real-time full scope simulator is modified by using a multiple-node model. In the new model, the pressurizer is divided into a number of control volumes. The vapor node consists of the control volumes where the vapor phase is continuous and liquid phase is dispersed, while each liquid node is a control volume where the liquid phase is continuous and vapor phase is dispersed. In the vapor node, the fluid is homogeneous and equilibrium, however, in any liquid node, the fluid is assumed to be in thermal equilibrium only. Liquid and vapor bubbles in the liquid node may have different velocity, and non-equilibrium exists among the liquid nodes and between the top liquid node and the vapor node.

The mass, momentum and energy equations for the vapor-liquid mixture are applied to the vapor node and each of the liquid nodes. To take into account the velocity difference between the vapor bubbles and the liquid in the liquid nodes, the slip ratio is modeled.

The new pressurizer module is integrated in the simulator. Some of the predictions from a number of transients are presented. The simulations are compared against available plant data and that of the previous two-node model. The comparisons show good agreement between the simulation by using the multiple-node model and the plant data. They also show significant improvements of the multiple-node model upon the two-node model.

1. INTRODUCTION

The training simulator at Point Lepreau has been playing an important role in training the Point Lepreau operators as well as the operators from other countries since 1991. Tremendous effort has been made to update the simulator software to meet the increasing training needs and to improve its fidelity.

Pressurizer is a key component in the plant, as well as in the simulator. Previously a two-node model is used in the simulator. In the two-node model, the vapor and liquid regions in the pressurizer are treated as two nodes. Each node is assumed homogeneous, respectively. Thermodynamic non-equilibrium exists between the vapor and the liquid node. The governing equations for the vapor and liquid node are solved.

The two-node model gives a reasonable prediction during very slow transients; however, erroneous predictions in pressure, level and temperature are reported frequently in relatively fast transients. The problems unveil the invalidity of the assumption that the liquid phase is homogeneous. In reality, the liquid in the pressurizer has a temperature distribution. The liquid and vapor bubbles in the liquid node have different velocities. Fail to simulate the temperature distribution and the vapor and liquid velocity differences affects the thermodynamic processes, which in turn affect the predictions for the pressurizer pressure, level and temperature.

There are various non-real-time pressurizer models with different complexities, ranging from the two-region model [1], two-region, four-state model [2], and three-region model [3] to non-equilibrium four-region model [4]. Under the real-time constrain, these models need to be modified such that the non-homogeneity between the liquid and vapor bubbles are reflected while the computing time is limited.

To simulate the behavior of the pressurizer liquid, the present work divides the pressurizer into a number of control volumes as shown in Figure 1.

The control volumes are occupied completely by either vapor phase (vapor with liquid droplets) or liquid phase (liquid with vapor bubbles), except in the control volume where the vapor phase interfaces with the liquid phase. This interfacing control volume may be partially occupied by the liquid phase, depending on the pressurizer level. The volumes occupied by the vapor phase is defined as a vapor node, while each control volume occupied by the liquid phase (completely or partially) is defined as a liquid node. Due to the dynamic nature of the pressurizer level, the number of the liquid nodes may change.

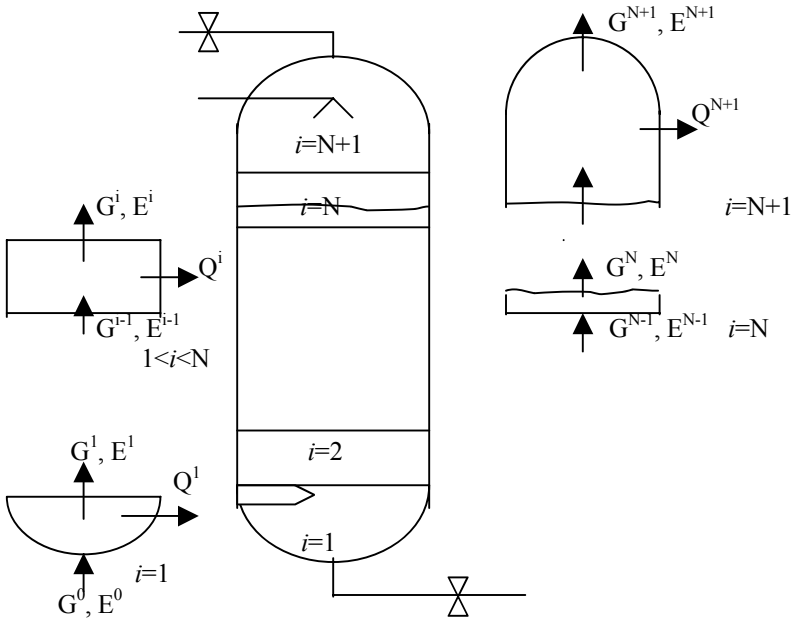

Fig 1. The pressurizer and its control volume

In the vapor node, the vapor and liquid droplets are homogeneous and they are in thermal equilibrium. In each liquid node, however the liquid and vapor bubbles are in thermal equilibrium. The two phases may have different velocity. Non-equilibrium exists among the liquid nodes, and between the topmost liquid node and the vapor node.

2. EQUATIONS OF THE MODEL

2.1 General Governing Equations

The parameters of the liquid nodes are assumed to be functions of time and height (z-direction, z=0 at the bottom of the pressurizer) only. Staggered grid approach used in CFD is adopted, i.e. the transport parameters are located on the surface of the nodes and the state parameters are located in the center of the nodes. In each liquid node, the vapor and liquid coexist as a mixture, and the discretized equation of continuity, energy and momentum for the mixture in the *i*th liquid node are written as [5]:

$$\partial_t M_m^i = A^i (G_m^{i-1} - G_m^i) \tag{1}$$

$$\partial_t H_m^i = A^i (E_m^{i-1} - E_m^i) + V^i (\partial_t P^i + h_{fg} \partial_t \Psi^i) + Q^i \tag{2}$$

$$L^i \partial_t G_m^i = \nu_m^{i-1} (G_m^{i-1})^2 - \nu_m^i (G_m^i)^2 + P^{i-1} - P^i - F^i / A^i + \rho_m^i g L^i \tag{3}$$

where $\partial_t=\partial/\partial t$, M_m^i ($\equiv\rho_m^i V^i$), ρ_m^i ($\equiv\alpha^i\rho_v^i+(1-\alpha^i)\rho_l^i$), G_m^i ($\equiv\alpha^i\rho_v^i u_v^i+(1-\alpha^i)\rho_l^i u_l^i=G_v^i+G_l^i$), H_m^i ($\equiv M_m^i h_m^i$), E_m^i ($\equiv G_m^i h_m^i$), h_m^i ($\equiv h_l^i+\chi^i(h_v^i-h_l^i)$), V^i ($\equiv A^i L^i$), Q^i, P^i, L^i and F^i are, respectively, the time derivative, the total mass, the mixture density, the mass flux, the total enthalpy, the energy flux due to mass flux, the specific collective enthalpy, the total volume, the heat transfer by conduction, the pressure, the height of the liquid and dispersed bubbles and the wall friction stress of the *i*th control volume. Ψ^i and ν^i are the slip correlation for the energy equation and effective specific volume for spatial acceleration, defined as:

$$\Psi^i \equiv \rho_l^i \chi^i (1-\alpha^i) + \rho_v^i (1-\chi^i)\alpha^i, \qquad \nu^i \equiv \frac{(\chi^i)^2}{\alpha^i \rho_v^i} + \frac{(1-\chi^i)^2}{(1-\alpha^i)\rho_l^i}$$

χ in the above expressions is the flow quality. It is defined by:

$$\chi^i \equiv \frac{W_v^i}{W_l^i + W_v^i} = \frac{\alpha^i \rho_v^i u_v^i}{\alpha^i \rho_v^i u_v^i + (1-\alpha^i)\rho_l^i u_l^i} = \frac{\alpha^i \rho_v^i}{\alpha^i \rho_v^i + (1-\alpha^i)\rho_l^i / S^i}$$

where S^i is the slip ratio ($\equiv u_v^i/u_l^i$)

For the vapor node, only Eqs. (1) and (2) are needed. The void fraction and flow quality of the vapor node are assumed to be one.

The index *i* ranges from 1 to N(t)+1, where N(t) is the number of the liquid nodes. For the convenience of computation, the bottommost liquid node is designated as the first liquid node (*i*=1), and all the pressurizer heaters are located inside this node. Thus for the topmost liquid node, *i*=N(t), and for the vapor node, *i*=N(t)+1.

The vapor pressure is prescribed by the equation of the state $P^{N+1}=P_v(\rho_v,h_v)$. By considering the size and the possible flow of the pressurizer, the pressure for each liquid node is approximated by:

$$P^N = P^{N+1} + \frac{1}{2} g \rho_m^N L^N \qquad P^{i-1} = P^i + \frac{g}{2}(\rho_m^i L^i + \rho_m^{i-1} L^{i-1})$$

To solve Eqs. (1-3) for the liquid nodes, the slip correlation, Ψ^i, the effective specific volume, ν^i, the wall friction stress F^i and the heat transfer Q^i for each node have to be determined.

The flow quality χ^i and void fraction α^i are the key parameters for Ψ^i and ν^i. The void fraction is determined from its propagation equation:

$$\partial_t \alpha^i = \Omega^i + u_\alpha^i(\alpha^i - \alpha^{i-1})/L^i \qquad (4)$$

By defining $C_0 \equiv <\alpha v>/<\alpha><v>$ ($<x> \equiv \int x dA/A$), $\Delta\rho \equiv \rho_l - \rho_v$, $\Gamma \equiv$the vapor generating rate and $u_{in}(t) \equiv$the fluid velocity entering the pressurizer, the expressions for Ω^i and u_α^i are obtained:

$$\Omega^i = [1 - C_0 \alpha^i \frac{\Delta\rho^i}{\rho_l^i}] \frac{\Gamma^i}{\rho_v^i}$$

$$u_\alpha^i = [C_0 u_{in}(t) + u_{vj}^i + \alpha^i \frac{\partial u_{vj}^i}{\partial \alpha} + \int_0^{z^i} \frac{C_0 \Delta\rho^i \Gamma^i}{\rho_l^i \rho_v^i} dz]$$

where u_{vj}^i is the drift velocity of vapor.

The most important variables in the expression of Ω^i and u_α^i are u_{vj}^i and Γ^i, and they are given, respectively by [6]:

$$u_{vj}^i = 1.53(1 - (\alpha^i)^2)[\frac{\sigma^i g(\rho_l^i - \rho_v^i)}{(\rho_l^i)^2}]^{1/4}$$

and [7]:

$$\Gamma^i = \frac{1}{h_{fg}^i}\{\frac{Q^i}{A^i} + \frac{dP^i}{dt}[1 - \rho_g^i \alpha^i (\frac{dh^i}{dP})_g - \rho_f^i (1 - \alpha^i)(\frac{dh^i}{dP})_f]\}$$

Using u_{vj}^i and Γ^i thus obtained in Ω^i and u_α^i, and then substituting the results into Eq. (4), we can compute the void fraction.

By definition, $u_{vj}^i = u_s^i(1-\alpha^i)$ [6], where $u_s^i = u_v^i - u_l^i$ is the slip velocity. So the slip velocity $u_v^i - u_l^i$ in each liquid node can be written as:

$$u_v^i - u_l^i = u_{vj}^i(1-\alpha^i)^{-1}$$

In the meantime, the sum of the volumetric flows of liquid and vapor at each node must be equal to the volumetric flow into the pressurizer as given by $v_0 = W_0/\rho_0$. Thus,

$$\alpha^i u_v^i + (1-\alpha^i)u_l^i = v_0 / A^i$$

Solving these two equations simultaneously results in the following slip ratio:

$$S^i \equiv \frac{u_v^i}{u_l^i} = \frac{v_0/A^i + u_{vj}^i}{v_0/A^i - \alpha^i(1-\alpha^i)^{-1}u_{vj}^i}$$

Based on the slip ratio and the nodal void fraction, the flow quality can be computed.

The volume of the topmost liquid node is a function of time. Because the sum of the volumes of the liquid nodes and the vapor node is the pressurizer total volume, $dV^{N+1} = -dV^N$ holds. dV^N can be determined from:

$$dV^N = \frac{dM^N}{\rho_m^N} - \frac{M^N}{(\rho_m^N)^2} d\rho_m^N = \frac{dM^N}{\rho_m^N} - \frac{V^N}{\rho_m^N}(\frac{\partial\rho_m^N}{\partial P} dP^N + \frac{\partial\rho_m^N}{\partial h} dh_m^N)$$

The friction and heat transfer are due to the presence of the boundaries. They are given in the next section.

2.2 Initial and Boundary Conditions

(2.2.1) *Initial conditions*

The initial values for vapor pressure and temperature, P^{N+1} and T^{N+1}, the pressurizer level and the liquid temperature at the first liquid node and the node located at z=8.46 meters are obtained directly from the plant data at 100% full power condition. By using these measurements, and assuming liquid enthalpy is a linear function of height initially, the initial values for the state parameter, M_m^i, ρ_m^i, H_m^i (i=1,2,… N(t)+1) can be calculated.

Since the thermal quality at ROHs are normally 0.4%, the initial void fraction in each liquid node is assumed to be 0.04.

The initial velocities for the vapor and liquid phase, the vapor generating rate in each liquid node are assumed to be equal to zero. Thus the transport parameters G_m^i, E_m^i, χ^i, ν^i and Ψ^i (i=1,2,..N(t)) can be calculated.

(2.2.2) *Boundary conditions*

The heat transfer (Q), the friction (F), the mass flux (G) and the energy flux (E) through the boundaries of the vapor node and each liquid node are specified in this section.

a. <u>For the vapor node (i=N(t)+1)</u>

As shown in Figure 1, the vapor is bounded by a.1-pressurizer wall, a.2- the steam relief line, a.3-cooling spray and a.4-the vapor-liquid interface.

<u>a.1</u> Heat is transferred from the vapor, through the pressurizer wall, to the environment. Associated with the heat transfer is the mass transfer from the wall to the topmost liquid node due to wall condensation.

The heat transfer from the vapor to the wall is calculated by:

$$Q_w^{N+1} = \pi D^{N+1} L^{N+1} C^{N+1} (T_m^{N+1} - T_w^{N+1})$$

where Q_w^{N+1}, D^{N+1} and C^{N+1} denote, respectively, the heat transfer from the vapor to the wall, the diameter and the heat transfer coefficient between vapor and the wall. T_m^{N+1} and T_w^{N+1} are the temperature of the vapor and the wall.

The wall temperature is determined by:

$$\frac{C_{p,w} M_w^{N+1}}{\pi D^{N+1} L^{N+1}} \frac{dT_w^{N+1}}{dt} = (C^{N+1} T_m^{N+1} + C_{w-e} T_e) - (C^{N+1} + C_{w-e}) T_w^{N+1}$$

where $C_{p,w}$, M_w, $C_{w\text{-}e}$, T_e denote, respectively, the wall specific heat, the vapor contacting wall mass, the heat transfer coefficient between the wall and environment and, the environment temperature.

Initially, vapor temperature is measured as 308°C, the wall temperature is assumed to be 300°C, the environment temperature is a constant of 30°C. The heat loss from the pressurizer steam space at 100% full power is approximately 15 kW. Based on these values, C^{N+1} and $C_{w\text{-}e}$ are determined. The vapor contact area and its contacting wall mass is dynamically computed as a function of pressurizer level, however, the heat transfer coefficients are assumed constant during all transients.

Based on Q_w^{N+1}, the wall condensation flow rate can be obtained as: $W_{condw}=Q_w^{N+1}/h_{fg}$. Thus the mass flux due to wall condensation is: $G_{m,w}^{N+1}=-G_{m,w}^{N}= W_{condw}/A^{N+1}$, and the associated energy flux is: $E_{m,w}^{N+1}=-E_{m,w}^{N}=G_{m,w}^{N+1}h_f$.

The wall friction, F_w^{N+1} is small and thus neglected.

<u>a.2</u> The conductive heat transfer through the steam relief line is assumed to be negligible, i.e.: $Q_r^{N+1}=0$. The friction on the steam relief line, F_r^{N+1} is small and thus neglected.

The steam discharge flow rate is calculated depending on if the flow is critical and pressurizer is full. When the pressurizer is not full, the vapor discharge flow is $W_r=C_{sd}\sqrt{(P_{prz}^2 - P_{dstrm}^2)}$ if the flow is not critical, or $W_r = C_{sd,crit} P_{prz}$ if the flow is critical. In this equation W_r represents the steam discharge flow rate, C_{sd} and $C_{sd,crit}$ denote, respectively, the non-critical and critical conductivity for the steam in the relief line, P_{dstrm} is the pressure at downstream. The mass flux due to steam relief is therefore $G_{m,r}^{N+1}=W_r/A^{N+1}$. The energy flux is $E_{m,r}^{N+1}=G_{m,r}^{N+1}h_v$. When the pressuriser is full, the fluid through the steam relief line is liquid. The discharge flow rate is then calculated by $W_r=C_{ld}\sqrt{(P_{prz} - P_{dstrm})}$ or $W_r = C_{ld,crit} P_{prz}$, where C_{ld} and $C_{ld,crit}$ represent, respectively the non-critical and critical conductivity for the liquid. The mass and energy flux are obtained from $G_{m,r}^{N}=W_r/A^{N}$ and $E_{m,r}^{N}=G_{m,r}^{N}h_l$ respectively.

a.3 When the pressurizer level is below the spray nozzles, the cooling spray condenses the vapor and brings vapor mass and its energy into the top liquid node. When the level is above the spray nozzles, the cooling spray is charged directly into the liquid node where the nozzles are located, and no vapor is condensed.

The conductive heat transfer through the spray line is assumed to be negligible, i.e.: $Q_s^{N+1}=0$. The friction on the spray nozzles, F_s^{N+1} is small and neglected.

When the pressurizer level is below the nozzle location, the spray flow rate is calculated by: $W_s = C_{sp}\sqrt{(P_{feed} - P^{N+1})}$ if the flow is non-critical, or $W_s = C_{sp,crit} P_{feed}$, if the flow is critical. The C_{sp} and $C_{sp,crit}$ in this equation denote the conductivity of the spray line when the flow is non-critical or critical, respectively.

The vapor condensation on the spray is expressed by:

$$W_{sc} = W_s(h_v - h_{sp})/(h_g - h_f)$$

where W_{sc} denotes the vapor condensation on the spray, and h_{sp} is the specific enthalpy of the spray flow.

The mass flux due to vapor condensation on the spray is therefore $G_{m,s}^{N+1}= W_{sc}/A^{N+1}$. The energy flux $E_{m,s}^{N+1}$ is obtained as: $G_{m,s}^{N+1}h_f$.

The spray, together with condensed vapor, directly falls into the topmost liquid node. So we have: $G_{m,s}^{N}= -(W_{sc}+W_s)/A^N$, $E_{m,s}^{N}= -(W_{sc}h_f+W_s h_{sp})/A^N$.

If the pressurizer level is at or above the nozzle's location (now the control volume becomes the *K*th liquid node), the spray flow rate is obtained by: $W_s = C_{spl}\sqrt{(P_{feed} - P^K)}$ if the flow is non-critical, or $W_s = C_{spl,crit} P_{feed}$, if the flow is critical. The mass flux is then $G_{m,s}^{K}= -W_s/A^K$, and the energy flux is $E_{m,s}^{K}=G_{m,s}^{K}h_s$.

a.4 On the liquid-vapor interface, there is mass and energy transfer through condensation of the vapor and evaporation of the liquid. Besides, there may be mass and energy transfer due to boiling and flashing.

The flow rate through the interface caused by the net effect of evaporation and condensation is modeled by [8]:

$$W_{ec} = C_{ec} A^N \left[\frac{P_s(T^N)}{\sqrt{T^N}} - \frac{P^{N+1}}{\sqrt{T^{N+1}}}\right]$$

where W_{ec} is the interfacial flow due to evaporation and condensation, $P_s(T^N)$ is the saturation pressure at temperature T^N. $C_{ec}=\sqrt{(M/(2\pi R))}$, where M is the molecular weight of D_2O and R is the universal gas constant.

Due to the change of the liquid enthalpy or pressure, boiling or flashing occurs. In time interval dt, the total flow through the interface caused by boiling or flashing is: $(\alpha^N A^N)(u_v^N dt)(\rho_v^N)$, thus the boiling and flashing flow rate is $W_{bf}=A^N\alpha^N\rho_v^N u_v^N$.

The total flow through the interface is the sum of the evaporation, condensation, boiling and flashing, i.e.: $W_i=W_{ec}+W_{bf}$. At any normal steady state, i.e. no leak of the vapor, the total interfacial flow must be equal to the flow of wall condensation, i.e.: $W_i=W_{condw}$. This property can be used to determine the vapor velocity in steady state.

Based on the interfacial flow, the interfacial mass flux is obtained as: $G_{m,i}^{N+1}=-G_{m,i}^{N}=-W_i/A^{N+1}$. When $W_i<0$, the mass is transferred from the vapor node to the topmost liquid node, so $E_{m,i}^{N+1}=-E_{m,i}^{N}=G_{m,i}^{N+1}h_f$. When $W_i>0$, however, the mass transfer is from the topmost liquid node to the vapor node, the energy flux is: $-E_{m,i}^{N+1}=E_{m,i}^{N}=G_{m,i}^{N}h_g$.

The conductive heat transfer through the interface is smaller compared with the energy transfer due to evaporation, condensation, boiling and flashing. So it is assumed to be zero. The friction on the interface, F_i^{N+1}, is also very small and neglected.

The total friction for the vapor is $F^{N+1}=0$. The total heat transfer to the vapor node is obtained as: $Q^{N+1}=-Q_w^{N+1}-Q_r^{N+1}-Q_s^{N+1}$. The total mass flux to the vapor node is obtained as: $G_m^{N+1}=G_{m,w}^{N+1}+G_{m,r}^{N+1}+G_{m,s}^{N+1}+G_{m,i}^{N+1}$, and the total energy flux is: $E_m^{N+1}=E_{m,w}^{N+1}+E_{m,r}^{N+1}+E_{m,s}^{N+1}+E_{m,i}^{N+1}$. Similarly, the total mass and energy flux through the boundaries to the topmost liquid node are, respectively $G_m^N=G_{m,w}^N+G_{m,r}^N+G_{m,s}^N+G_{m,i}^N$ and $E_m^N=E_{m,w}^N+E_{m,r}^N+E_{m,s}^N+E_{m,i}^N$.

b. For the liquid nodes (*i*=1,2,…,N)

Except for the topmost (*i*=N) and the bottommost one (*i*=1), the liquid nodes (*i*=2,…,N-1) are only bounded by b.1- the pressurizer wall in their periphery. To the topmost liquid node, it is also bounded by b.2- its upper surface, and to the bottommost one, by b.3-its lower surface.

b.1 The heat transfer from the liquid to the wall is calculated by:

$$Q_w^i = \pi D^i L^i C^i (T_m^i - T_w^i), \quad (i=1,2,\ldots,N)$$

where Q_w^i, D^i and C^i denote, respectively, the heat transfer from the liquid to the wall, the diameter and the heat transfer coefficient between liquid and the wall. T_m^i and T_w^i are the temperature of the liquid-vapor bubble mixture and the wall, respectively.

The wall temperature for each liquid node is calculated from:

$$\frac{C_{p,w}M_w^i}{\pi D^i L^i}\frac{dT_w^i}{dt} = (C^i T_m^i + C_{w-e}T_e) - (C^i + C_{w-e})T_w^i$$

No heat generation exists in the liquid nodes, except in the first one. Hence $Q^i=-Q_w^i$ (i=2,…,N). In the first liquid node, the heat generated by pressurizer heaters is given by $Q_{in}(t)$ the heat transfer to the first node is therefore $Q^1=Q_{in}(t)-Q_w^1$.

There is no mass transfer through the wall. The wall friction for the liquid nodes are obtained as:

$$F^i = \pi D^i L^i \left(\frac{f^i L^i}{D^i} + K^i\right)\phi_{lo}\frac{(G_l^i)^2}{\rho_l^i} \qquad (i=1,2,\ldots,N)$$

where f^i, K^i, ϕ_{lo}, G_l^i are, respectively, the friction factor, the form loss coefficient, the two-phase multiplier and the liquid mass flux.

The friction factor is computed by using $f^i=aR_e^{-b}$, a and b are constants depending on R_e. Typical values for a and b can be found in [4]. Because the pressurizer is a large vertical vessel, the form loss coefficient can be set to zero.

Friedel correlation is used to compute two-phase multiplier ϕ_{lo}.

b.2 To the Nth (topmost) liquid node, the flow across its upper face are the interfacial flow given in a.1 and a.4. The friction on the upper surface is very small and thus neglected.

b.3 To the first (bottommost) liquid node, the flow across its lower face is given by another subroutine as $W_0=A^0[(1-\alpha^0)\rho_f^0+\alpha^0\rho_v^0]u_{in}$. The mass velocity and energy flux can be obtained as: $G_m^0=W_0/A^1$ and $E_m^0=G_m^0 h_0$.

3. THE TESTS OF THE MODEL

3.1 The computational procedure

Eqs. (1-4) and their supplemental equations are solved for each node by following the procedure below.

(3.1.a) computing G, E and Q through the liquid-vapor interface.
(3.1.b) computing vapor mass and enthalpy from Eqs. (1) and (2).
(3.1.c) computing vapor density and specific enthalpy by using the previous vapor node volume.
(3.1.d) determining vapor pressure by using vapor density and specific enthalpy.
(3.1.e) computing the vapor generating rate Γ^i.
(3.1.f) computing the vapor drift velocity u_{vj}^i.
(3.1.g) computing Ω^i and u_α^i.
(3.1.h) computing the void fraction α^i from Eq. (4)
(3.1.i) computing the wall heat transfer Q^i, the wall friction F^i, the node pressure P^i, the slip ratio S^i, the flow quality χ^i, the specific volume for spatial acceleration v^i and finally, the slip correlation for the energy equation Ψ^i.
(3.1.j) computing the mass flux, G_m^i, the node mass M_m^i and the node enthalpy, H_m^i from Eq. (3), (1) and (2).
(3.1.k) computing mixture density and specific enthalpy by using the node volume (constant, except for node-N and N+1 of which volumes are computed after determining dV^N and dV^{N+1}).

3.2 The test environment

The set of equations introduced above are solved in a subroutine. The subroutine is linked with the other system subroutines, and they are built into the Point Lepreau real-time simulator. All the subroutines dynamically interact

with each other. They also interact with the plant digital control computer (DCC) programs, the plant control logic and the main control room operators.

3.3 The simulation results and discussions

Test 1. Steady state and power maneuvering

The aim of this test is to evaluate the overall calculation of the mass and energy conservation in the pressurizer, and the interaction of the pressurizer with the other primary heat transport systems.

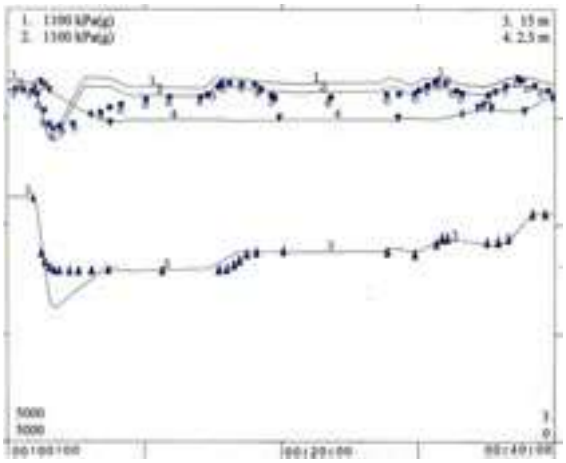

Fig. 2 The pressure and level response
1. PROH5 (■, Plant data), 2. PPRZ (o, Plant data), 3. LPRZ (▲, Plant data), 4. LSTO (▼, Plant data)

In this test the reactor power is first maintained at 100% full power. Then the power is reduced to 77% full power and back to 100% full power again at different rate.

The steps outlined in (3.1.a) to (3.1.k) are repeated until all the parameters become visually stable. This steady state is stored in the memory and is named 100%FP steady state. Figure 2 shows the pressurizer steam pressure, PPRZ, the pressurizer liquid level, LPRZ, the reactor outlet header 5 pressure, PROH5 and the D2O storage tank level, LSTO, at 100%FP steady state at the beginning of the test. The predictions of the simulator for these parameters at 100%FP by using the multiple-node model are in a good agreement with the plant data. The average of the D2O storage tank level is a constant, which indicates that the total mass in the primary heat transport system is constant. The mass conservation of the pressurizer liquid is achieved since the pressurizer level is a constant as shown in Figure 2. The conservation of the mass of the pressurizer vapor is reflected by Figure 3, which shows that the interface mass flux is equal to the vapor wall condensation rate, hence the vapor mass conservation is also achieved.

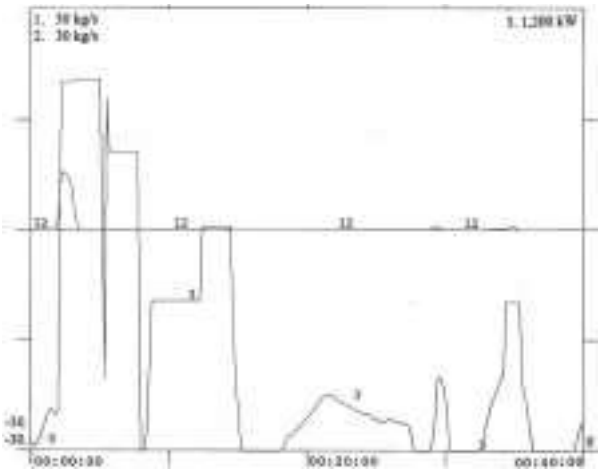

Fig.3 Evaporation, condensation and heaters

1. Wall condensation flow, 2. Interface flow, 3. Heater output

The reactor power is then manually reduced at a rate of -0.25%/s to 77% full power. Because the DCC program is controlling the reactor outlet head pressure, the pressurizer heaters are turned on automatically to restore the PROH5 as shown in Figure 3. The PROH5 decreases and then recovers. Due to the deficiency in the subroutine for the boilers, the simulator predicts a lower minimum pressurizer level and pressure, but a faster pressure recovery than that in the plant. This occurs in the first 10 minutes of the test as can be seen in Figure 2. After 10 minutes, the pressures and level are in a good agreement with the plant data. Figure 3 shows that, when the pressurizer pressure is reduced, the DCC program turns on all the heaters, and there is a sharp increase in mass transfer due to boiling and flashing. The interface flow declines as the pressurizer pressure starts to recover. Finally, the interface flow balances with the wall condensation flow again.

After the heat transport system becomes stable, the reactor power is then manually increased from 77% to 100% in three stages, namely, from 77% to 90% at a rate of +0.1%/s, from 90% to 95% at a rate of 0.05%/s and from 95% to 100% at a rate of 0.025%/s at 17.5 minutes.

When the power increases, pressure begins to increase, as indicated in Figure 2. The pressurizer level also starts to increase and the vapor in the vapor node is gradually compressed. So the vapor temperature rises above the saturation. The multiple-node model predicts a temperature distribution in liquid. Figure 4 shows the temperature at node-1 (bottom) and node-8 (middle). The liquid temperature at node-8 increases due to the heat transfer from the vapor. The temperature at node-1 decreases due to the in-surge of the relatively cooled water from the reactor outlet header. The temperature gaps among the liquid node shrink because of the liquid convection. The simulation of this phenomenon is crucial to the prediction of the interface mass flux and the vapor pressure. Unfortunately, the two-node model is not able to capture this phenomenon.

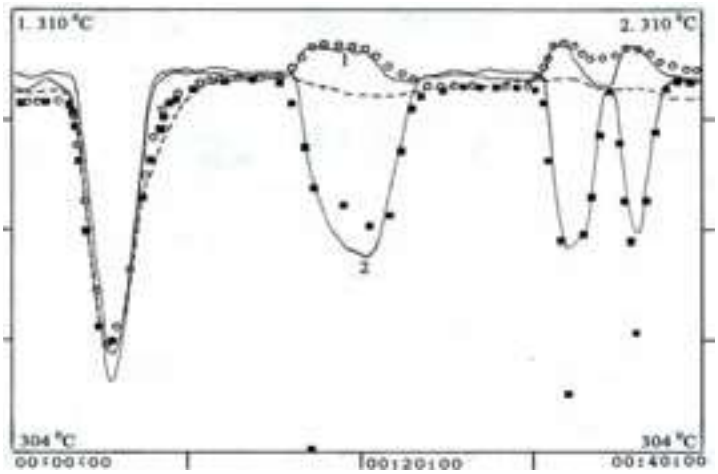

Fig. 4 Temperature response

1. Temperature at the middle of the pressurizer (o, Plant data, -----, Two-node model)
2. Temperature at the bottom of the pressurizer (■, Plant data, -----, Two-node model)

Test 2. Reactor trip at 100% full power

The reactor trip is an important transient. The aim of this test is to further verify the multiple-node model.

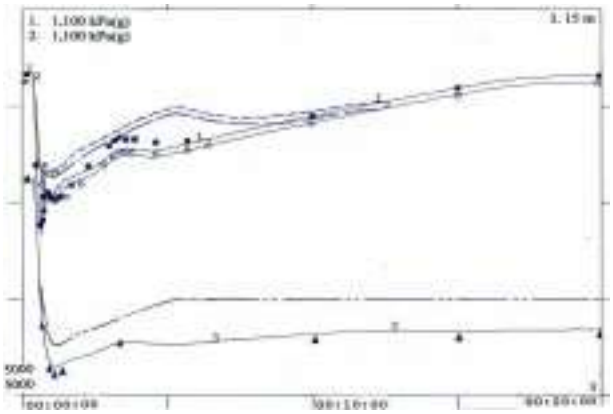

Fig. 5 The pressure and level response

1. PROH5 (■, Plant data, --, Two-node model), 2. PPRZ (o, Plant data, —·—, Two-node model),
3. LPRZ (▲, Plant data, —- -—, Two-node model),

When the reactor trips at 100% full power, the pressurizer level and the PHT system pressure decrease suddenly due to the shrink of the primary heat transport system. As shown in Figure 5, the pressure at ROH5 drops to 7.2Mpa(g), and the pressurizer level, to 3.4M in the plant. The simulation by using the multiple-node model, predicts a minimum ROH5 pressure of 7.2Mpa(g) and a minimum pressurizer level of 3.5m. These predictions are in very good agreement with the plant data, and they are better than that of the simulation using the two-node model, which predicts a minimum ROH5 pressure of 6.9Mpa(g) and a level of 4.5M.

About 1 minute after the trip, the pressurizer pressure, the pressurizer level and the pressure at ROH5 start to recover. Figure 5 shows that the pressure and level recovery predicted by the multiple-node model simulation are very close to the plant data, and they improved the predictions of the two-node model simulation.

Test 3. Total loss of Instrument air

The purpose of this test is to compare the heat transport pressure predicted by the simulator using the multiple-node model with that using the two-node model. It is realized that the pressure in the heat transport system becomes crucial to the operators in this scenario.

Due to the loss of the instrument air, the heat transport system D_2O feed valves open fully and the bleed valves close. Meanwhile, the pressurizer steam relief valves close. There is a net mass increase in the primary heat transport system. The extra mass enters the pressurizer, resulting in an increase in the pressurizer level. The pressurizer steam space is compressed. The vapor pressure and the heat transport system pressure increase. This can be seen in Figure 6.

The larger boiler feed water valves also close because of no instrument air. The reactor finally trips on low boiler level. Due to the reactor trip, the primary heat transport system shrinks. The pressurizer level and pressure decrease sharply due to a large flow out-surge caused by the reactor trip. As can be seen from Figure 6, the pressure at the ROH predicted by the simulator using the multiple-node model is lower than that using the two-node model by 450Kpa, and the pressurizer pressure, by 150Kpa.

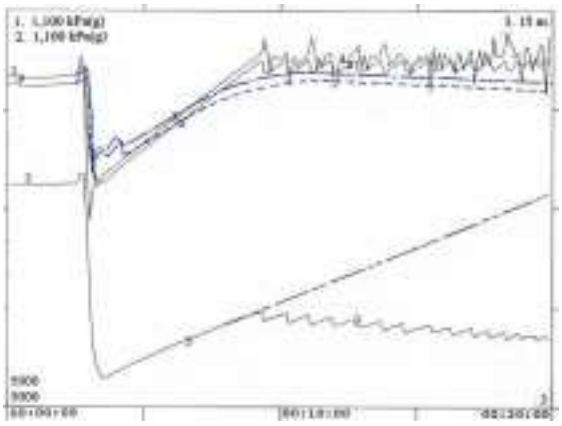

Fig 6. ROH3 pressure and pressurizer pressure and level response

1. PROH3 (— · —, Two-node model), 2. PPRZ (-------, Two-node model), 3. LPRZ (— - -—, Two-node model).

Because the feed pump is continuously supplies the liquid into the PHT system, the pressurizer level increase again after it drops. The rate of the pressure increase in the multiple-node model is larger than that in the two-node model. This is judged to be more realistic and supported by Figure 7.

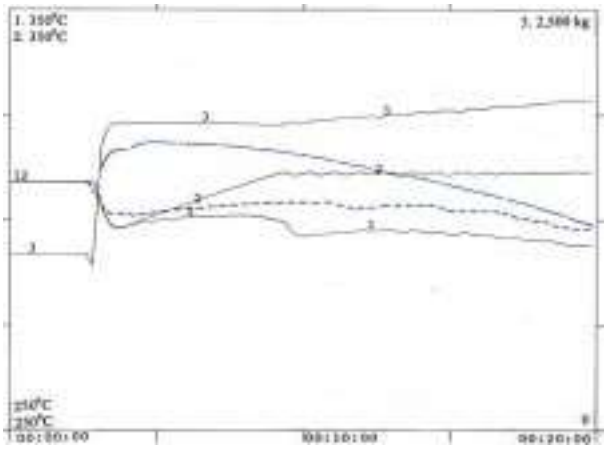

Fig 7. The temperature and vapor mass in pressurizer

1. Temperature at the bottom of the pressurizer (-----, Two-node model)
2. Temperature at the middle of the pressurizer (-----, Two-node model),
3. Vapor mass (— · —, Two-node model).

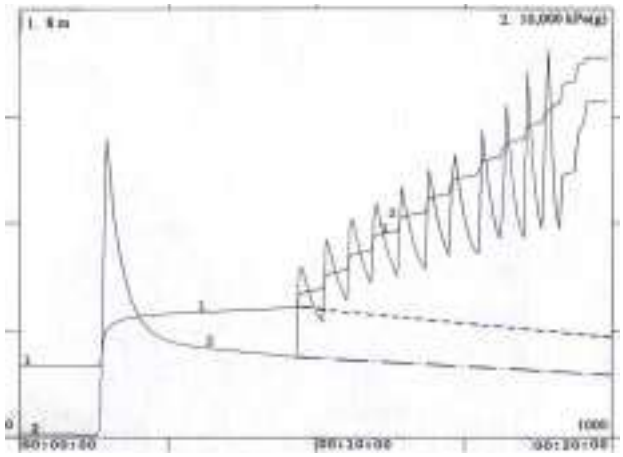

Fig. 8 The degasser condenser level and pressure response

1. The degasser level (-----, Two-node model), 2. The degasser pressure (— · —, Two-node model).

At the end of the reactor trip, the reactor outlet temperature dropped to a value, which is lower than the pressurizer temperature. When the liquid mass enter the pressurizer again, the incoming liquid is cooler than the liquid in the

pressurizer. The liquid at the bottom of the pressurizer (node-1) will be affected by the incoming cold liquid much more than the liquid at the immediately below the interface (node-N). It can be seen in Figure 7 that the liquid temperature has a distribution as predicted by the multiple-node model.

As the liquid continuously goes to the pressurizer, the pressurizer steam space is compressed, and the steam pressure and temperature increase, resulting in an increase in wall condensation. In the multiple-node model, the liquid at node-N become hotter and hotter due to the vaporization of the liquid below and the condensation of the vapor above. The mass flux through the interface from node-N to node-(N+1) increases. The total effect of the wall condensation of vapor and the evaporation of the liquid in node-N is that the vapor mass is almost a constant, but the vapor pressure and liquid level increase continuously. In the two-node model, however, the temperature of the liquid below the interface is lower than that in the multiple-node model, therefore the evaporation rate of the liquid is not large enough to balance the vapor wall condensation, hence a reduction of the vapor mass is predicted. Because the pressure is a function of the density, which in turn depends on the mass and volume, the pressure in the two-node model increases in the first 10 minutes due to the decrease of vapor volume. After 10 minutes, the rate of decrease of the vapor mass excesses the rate of decrease of the volume, resulting in an decrease of the vapor density and an decrease of vapor pressure.

The pressurizer pressure in the multiple-node model increases so high, resulting in the opening of the liquid relief valves. Coolant in the PHT systems is then discharged into the degasser condenser. It can be seen from Figure 8 that the degasser condenser is filled very quickly, and the PHT system becomes solid. This phenomenon is so important to the control room operators. To avoid the opening of the liquid relieve valves and filling of the degasser condenser, certain procedures have to be followed. In the two-node model, however, the pressure is never be able to open the liquid relief valves, and finally it becomes stable. This may mislead the operator into overlooking the difficulty of the pressure control after the incident.

4. CONCLUDING REMARKS

The multiple-node pressurizer model has been tested on the full scope simulator at Point Lepreau Station. The introduce of the multiple nodes into the liquid phase improves the predictions for the liquid temperature, the interface mass flux. Thus it improves the prediction of the pressure in the pressurizer as well as in the primary heat transport system, especially during an in-surge transient.

The tests indicate that, in a slow transient, the assumption of the liquid homogeneity is acceptable. During a fast transient, however, the liquid is not homogeneous and inhomogeneity should be properly taken into account.

5. ACKNOWLEDGMENT

The effort of Mr. D. Parker, the supervisor of refresh training, in testing the multiple-node model is very much appreciated.

6. REFERENCES

[1] EPRI Inc.: "RETRAN-02, A Program for Transient Thermal-Hydraulic Analysis of Complex Fluid Flow System", Idaho (1984)
[2] V.V. Athani and L. Vijaykumar: “Digital Simulation of the Pressurizer in a Pressurized Water Nuclear Reactor”, Nuclear Technology, V. 61, p. 547 (1983)
[3] S.N. Kim and P. Griffith: “PWR Pressurizer Modeling”, Nuclear Eng. Design. V. 102, p. 199 (1987)
[4] N.E. Todreas and M.S. Kazimi: "Nuclear Systems I", Hemisphere Pub. Corp., New York (1990)
[5] L.S. Tong: "Boiling Heat Transfer and Two-Phase Flow", John Wiley & Sons, Inc., Publishers, New York (1964)
[6] G. B. Wallis: “One Dimensional Two-Phase Flow”, McGraw-Hill Book Company, New York (1969)
[7] G. Inagatullah, W.T. Hancox and W.B. Nicoll: “Prediction of the vapor volumetric fraction in flow boiling during pressure decay: An analytical approach”, AICHE Symp. Series, Heat Transfer: Research and Application, No. 174 V. 74 (1975)
[8] J.G. Collier: “Convective Boiling and Condensation”, 2nd ed. McGraw-Hill Book Company, New York (1972)